Developmental Biology **232,** 301–314 (2001)
doi:10.1006/dbio.2001.0187, available online at http://www.idealibrary.com on IDEAL®

Mesenchymal Factor Bone Morphogenetic Protein 4 Restricts Ductal Budding and Branching Morphogenesis in the Developing Prostate

Marilyn L. G. Lamm, Carol A. Podlasek, Daniel H. Barnett, Juliet Lee, J. Quentin Clemens, Christy M. Hebner, and Wade Bushman[1]

Department of Urology, Northwestern University Medical School, Tarry Building 11-715, 303 E. Chicago Avenue, Chicago, Illinois 60611

The budding of the urogenital sinus epithelium into the surrounding mesenchyme signals the onset of prostate morphogenesis. The epithelial and mesenchymal factors that regulate ductal budding and the ensuing process of ductal growth and branching are not fully known. We provide evidence that bone morphogenetic protein 4 (BMP4) is a mesenchymal factor that regulates ductal morphogenesis. The *Bmp4* gene was most highly expressed in the male urogenital sinus from embryonic day 14 through birth, a period marked by formation of main prostatic ducts and initiation of ductal branching. From an initial wide distribution throughout the prostatic anlage of the urogenital sinus, *Bmp4* expression became progressively restricted to the mesenchyme immediately surrounding the nascent prostatic ducts and branches. Exogenous BMP4 inhibited epithelial cell proliferation and exhibited a dose-dependent inhibition of ductal budding in urogenital sinus tissues cultured *in vitro*. Adult *Bmp4* haploinsufficient mice exhibited an increased number of duct tips in both the ventral prostate and coagulating gland. Taken together, our data indicate that BMP4 is a urogenital sinus mesenchymal factor that restricts prostate ductal budding and branching morphogenesis.

Key Words: **bone morphogenetic protein 4; prostate development; branching morphogenesis.**

INTRODUCTION

The accessory male sex organs include both Wolffian duct derivatives (epididymis, ductus deferens, ampullary gland, and seminal vesicle) and urogenital sinus derivatives (prostate and bulbourethral gland). The adult mouse prostate is an exocrine gland comprised of three paired lobes: anterior (also called the coagulating gland), dorsal, and ventral. Each lobe consists of a highly branched ductal network connected to the urethral lumen by multiple main ducts (Cunha and Lung, 1979; Cunha *et al.*, 1987).

The embryonic precursor of the prostate, the prostatic anlage, develops from the cranial portion of the urogenital sinus and consists of a multilayered epithelium surrounded by mesenchyme (Cunha and Lung, 1979). The first morphological change indicative of prostate development occurs with outgrowths of the urogenital sinus epithelium into the surrounding mesenchyme to form epithelial buds that will become the main prostatic ducts. In the mouse, prostatic bud formation begins at embryonic day 17 (E17: 20-day gestation period) and continues throughout the perinatal period (Cunha *et al.*, 1987). Elongation and branching of the main ducts begin prenatally but occur most intensively during the first 15 days of postnatal life (Sugimura *et al.*, 1986). Differences in temporal and spatial patterns of ductal branching produce the distinctive ductal architectures that characterize the three prostate lobes (Lung and Cunha, 1981; Sugimura *et al.*, 1986).

Prostate development requires testosterone. Androgens bind receptors in the urogenital sinus mesenchyme and are postulated to induce ductal morphogenesis by promoting mesenchymal–epithelial interactions (Cunha *et al.*, 1987). Several growth factors have been proposed as regulators of prostate development. *Epidermal growth factor* (*EGF*) and *transforming growth factor-α* (*TGF-α*) are both expressed in rodent prostate (Haughney *et al.*, 1998) and *TGF-α* overexpression causes hyperplasia of the adult coagulating gland (Sandgren *et al.*, 1990), but there is no evidence that either EGF or TGF-α are required for prostate development. *Ker-*

[1] To whom correspondence should be addressed. Fax: (312) 908-7275. E-mail: w-bushman@northwestern.edu.

0012-1606/01 $35.00

atinocyte growth factor (*Kgf*, also known as *Fgf7*) is expressed in the urogenital mesenchyme (Finch *et al.*, 1995; Thomson *et al.*, 1997). KGF stimulates proliferation of prostatic cells (Yan *et al.*, 1992), promotes prostatic branching *in vitro* (Sugimura *et al.*, 1996; Thomson *et al.*, 1997), and causes prostate hyperplasia when overexpressed in transgenic mice (Kitsberg and Leder, 1996). However, transgenic loss of KGF function does not cause morphological abnormalities in the reproductive tract of the adult male (Guo *et al.*, 1996). *Fibroblast growth factor 10* (*Fgf10*) is expressed in the urogenital mesenchyme and FGF10 stimulates growth and branching of neonatal ventral prostate *in vitro* in the absence of testosterone (Thomson and Cunha, 1999). *Transforming growth factor-β1* (*TGF-β1*) is expressed in the developing prostate (Timme *et al.*, 1994; Itoh *et al.*, 1998). TGF-β1 inhibits proliferation of prostatic cells *in vitro* (Martikainen *et al.*, 1990; Wilding, 1991) and inhibits testosterone's stimulatory effect on prostatic ductal morphogenesis *in vitro* (Itoh *et al.*, 1998).

Bone morphogenetic protein 4 (*Bmp4*) is a member of the *TGF-β* superfamily (Wozney *et al.*, 1988) and is the vertebrate homolog of the *Drosophila* gene *decapentaplegic* (Gelbart, 1989). *Bmp4* transcripts are found in regions of the developing limb, lung, kidney, whisker follicle, and tooth bud where inductive interactions occur between mesenchyme and adjacent epithelium, and BMP4 has been implicated in the morphogenesis of these organ systems (Bitgood and McMahon, 1995; Hogan, 1996). A regulatory role for BMP4 in developmental systems that involve budding and branching morphogenesis has received particular attention. BMP4 disrupted branching morphogenesis in embryonic lung and kidney (Bellusci *et al.*, 1996; Raatikainen-Ahokas *et al.*, 2000). The expression of *Bmp4* was recently reported in adult human, rat, and mouse prostate (Harris *et al.*, 1994; Thomas *et al.*, 1998) but the role of BMP4 in prostatic bud formation and branching has not been previously investigated.

In this study, we show a dynamic pattern of *Bmp4* expression in the embryonic prostate that shifts from an initial wide domain in the prostatic anlage of the urogenital sinus to a restricted zone of mesenchyme immediately surrounding the emerging prostatic epithelial buds. Using a combination of *in vitro* culture of embryonic urogenital sinus tissues and quantitative analysis of the prostatic ductal network of a previously generated *Bmp4* haploinsufficient mutant mouse (Dunn *et al.*, 1997), we demonstrate that BMP4 inhibits epithelial cell proliferation in the urogenital sinus and provide evidence that in the developing prostate BMP4 functions to restrict prostatic ductal budding and inhibit ductal branching.

MATERIALS AND METHODS

Tissue Collection

Urogenital sinus and prostate tissues were obtained from either BALB/c (Jackson Laboratories, Bar Harbor, ME) or CD-1 (Charles River Laboratories, Wilmington, MA) mice. The day of vaginal plug was designated embryonic day 0 (E0) and the day of birth was designated P1. Adult C57BL/6J-$A^{w\text{-}J}$-Ta^{6J}+/+Ar^{Tfm} mice with mutant androgen receptors (*Tfm*, testicular feminization) and C57BL/6-$Bmp4^{tm1Blh}$ mice were obtained from Jackson Laboratories. Tissues were dissected as previously described (Oefelein *et al.*, 1996; Podlasek *et al.*, 1997). Separation of epithelial and mesenchymal tissues from intact E16 urogenital sinus was performed as described previously (Cunha and Donjacour, 1987).

RNA Isolation and RT-PCR

Total RNA was isolated from either pooled or individual specimens using the TRIzol method (Life Technologies, Gaithersburg, MD) as described previously (Podlasek *et al.*, 1997). Semiquantitative RT-PCR was performed with 29 or 32 cycles of amplification (RT-PCR Core Kit; Perkin–Elmer, Foster City, CA). Reactions were routinely performed without reverse transcriptase to demonstrate RNA dependence of reaction products. Quantitative RT-PCR (QRT-PCR) was performed by determining the ratio between the products for *Bmp4* and for ribosomal subunit *RPL-19* that was used as an endogenous internal standard. RT-PCR was performed over a range of cycle number (22–32 cycles) on 50 ng of total RNA as described previously (Podlasek *et al.*, 1999a,c). Densitometry of the photographed gel was performed using the Bio-Rad Molecular Analyst (Bio-Rad, Richmond, CA). The log of band density versus cycle number was plotted and the ratio of the products within the linear range was determined. *RPL-19* yields a 556-bp product. *Bmp4* yields a 235-bp product that was confirmed by restriction digestion with two enzymes *Sac*I and *Apa*I. *Shh* yields a 260-bp product that was confirmed by restriction digestion with *Msp*I and *Hae*III. *BMPR-IA* yields a 233-bp product that was confirmed by restriction digestion with *Pvu*II and *Nco*I. *BMPR-IB* yields a 292-bp product that was confirmed by restriction digestion with *Ava*I and *Sac*I.

RT-PCR primer sequences 5′–3′ were: *Bmp4* antisense, TCCAGGAACCATTTCTGCTG; *Bmp4* sense, CACTGTGAGGAGTTTCCATC; *Bmp2* antisense, TGAGTGCCTGCGGTACAGAT; *Bmp2* sense, TGTCTTCTAGTGTTGCTGCT; *RPL-19* antisense, GGAAGAGTCTTGATGATCTC; *RPL-19* sense, CTCAGGCTACAGAAGAGGCTT; *Shh* antisense, ACTGCTCGACCCTCATAGTG; *Shh* sense, GGCAGATATGAAGGGAAGAT; *BMPR-1A* antisense, GGTTGTGCTCATTTCCATGG; *BMPR-1A* sense, TGGCAATAGTTCGCTGAACC; *BMPR-1B* antisense, TAGCGGCCTTTTCCAATCTG; *BMPR-1B* sense, TTGTTGATGGGCCCATACAC.

Probe Synthesis

A full-length (1550-bp) *Bmp4* cDNA cloned into pSP72 was provided by Dr. Hogan (Vanderbilt University Medical Center, Nashville, TN). The CsCl-purified plasmid was linearized with *Acc*I (antisense) and *Eco*RV (sense). Probes were prepared using a DIG RNA labeling kit (Roche Molecular Biochemicals, Indianapolis, IN) and appropriate T7 and SP6 RNA polymerases. Concentrations of antisense and sense riboprobes, quantitated by spotting dilutions on nitrocellulose paper along with control DIG-RNA, were about 2 μg/μl.

Whole-Mount in Situ Hybridization

In situ hybridization of 4% paraformaldehyde-fixed urogenital tissues was performed according to a previously described protocol

(Wilkinson, 1992). Briefly, tissues were bleached with 6% hydrogen peroxide (60 min), digested with 10 μg/ml proteinase K (15 min), and refixed in 0.2% glutaraldehyde/4% paraformaldehyde (20 min) at room temperature. Hybridization with digoxygenin-labeled RNA probes for *Bmp4* (1 μg/ml) was performed at 70°C for 16 h. Following high stringency washes and RNAse treatment, tissues were incubated with an alkaline phosphatase-coupled anti-digoxygenin antibody (Roche Molecular Biochemicals) for 16 h at 4°C. The color reaction was developed using nitroblue tetrazolium and 5-bromo-4-chloro-3-indolyl phosphate as substrates. Some stained tissues were incubated in 50% sucrose/phosphate buffered saline (PBS) solution at 4°C overnight, embedded in Tissue-Tek OCT compound and cryosectioned at 15 μm.

In Vitro Organ Culture

Culture of male urogenital sinus obtained at E15 and E17 was performed as previously described (Cooke *et al.*, 1987). Tissues were isolated from the bladder, distal urethra, and Wolffian and Mullerian ducts and transferred to 0.4 μm Millicell-CM filters (Millipore Corp., Bedford, MA) placed inside six-well tissue plates. Each well contained 1.5 ml serum-free DMEM:Ham's F-12 (1:1) supplemented with 2% ITS (12.5 μg/ml insulin, 12.5 μg/ml transferrin, 12.5 ng/ml selenious acid, 2.5 mg/ml bovine serum albumin, and 10.7 μg/ml linoleic acid; Collaborative Biomedical Products, Bedford, MA), 25 μg/ml gentamycin, 0.25 μg/ml amphotericin B, and 10^{-8} M dihydrotestosterone (DHT) dissolved in 95% ethanol. In DHT-free media, ethanol was added to a final concentration of 0.1%. Cultures were maintained in a humidified 37°C, 5% CO_2 incubator.

BMP4 Bead Experiments on Cell Proliferation

Recombinant human (rh) BMP4 protein was supplied by Genetics Institute (Cambridge, MA). Agarose beads (100–200 μm diameter; Bio-Rad) were incubated in BMP4 solution (37.5 μg/ml) or PBS for 1 h at room temperature. One to four beads were placed on each urogenital sinus at the mesenchymal–epithelial interface of the prostatic anlage. Tissues were maintained in serum-free, DHT-supplemented culture medium as described above. Following 48 h of culture, bromodeoxyuridine (BrdU) staining of tissues was performed using an *in situ* proliferation kit according to the manufacturer's protocol (Roche Molecular Biochemicals). BrdU uptake in formalin-fixed sectioned tissues was visualized following incubation with anti-BrdU-alkaline phosphatase-conjugated antibody. For quantitative analysis of BrdU staining, all fields containing BMP4 or control beads were examined under one high-power field at ×40 magnification within an area of 1.4 mm^2 with the bead in the center of the field. Stained epithelial and mesenchymal cells within this area were counted and BrdU labeling indices (number of stained nuclei/total number of nuclei counted = % labeled) were determined. The proportions of stained nuclei in control and BMP4-treated sections were analyzed using chi-square test. Adjacent sections were processed for TUNEL staining to detect cell death using the *in situ* apoptosis detection kit according to the manufacturer's directions (Trevigen Inc., Gaithersburg, MD).

Morphologic Analysis of Heterozygous Bmp4 Mutant Mice

Construction of the targeting vector and generation of chimeras and colonies of mice heterozygous for the $Bmp4^{tm1Blh}$ targeted allele was previously described (Winnier *et al.*, 1995). Adult heterozygous $Bmp4^{tm1Blh}$ mutants and wildtype (C57BL/6J) animals were obtained from Jackson Laboratories. Qualitative and quantitative analyses of main ducts (n = 5 wildtype and 5 mutant mice) and duct tips (n = 9 wildtype and 10 mutant mice) in prostatic lobes were performed in a blinded manner as previously described (Podlasek *et al.*, 1997). Quantitative microdissection of individual prostatic lobes and counting of the duct tips as a measure of ductal branching were performed as previously described (Sugimura *et al.*, 1986; Podlasek *et al.*, 1997). Statistical analysis of differences was performed using unpaired *t* test.

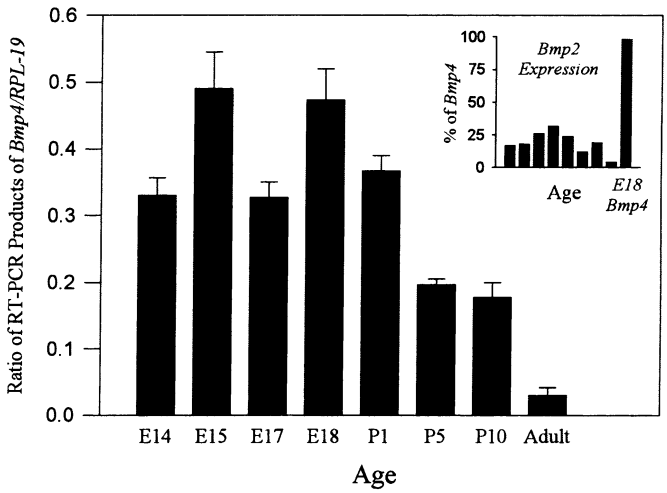

FIG. 1. Time course of *Bmp4* expression in the urogenital sinus and developing prostate as determined by QRT-PCR utilizing the message for ribosomal subunit *RPL-19* as an internal standard. Each bar represents the mean ± SEM of triplicate assays of RNA from pooled tissues at each time point. Figure inset shows time course of *Bmp2* expression determined by QRT-PCR at the same time points as that used for *Bmp4*. A comparison of *Bmp2* and *Bmp4* expression was made by using the same internal standard for both reactions and normalizing *Bmp2* expression to the expression of *Bmp4* at E18. Each bar represents the mean ± SEM of duplicate assays of RNA from pooled tissues at each time point.

RESULTS

Bmp4 Expression during Prostate Development

The time course of *Bmp4* expression in the developing prostate was determined by QRT-PCR (Fig. 1). *Bmp4* expression was generally high in the urogenital sinus from E14 through P1. Expression significantly decreased in the postnatal period (P5, P10) and declined to an even lower level in the adult. The overall level of *Bmp4* expression in the coagulating gland, ventral prostate, and dorsal prostate was compared by QRT-PCR at P5, the earliest time point at which the different lobes can be cleanly separated. The level of *Bmp4* expression was similar in all three lobes (data not shown). The *Bmp4* homolog *Bmp2* is also expressed in

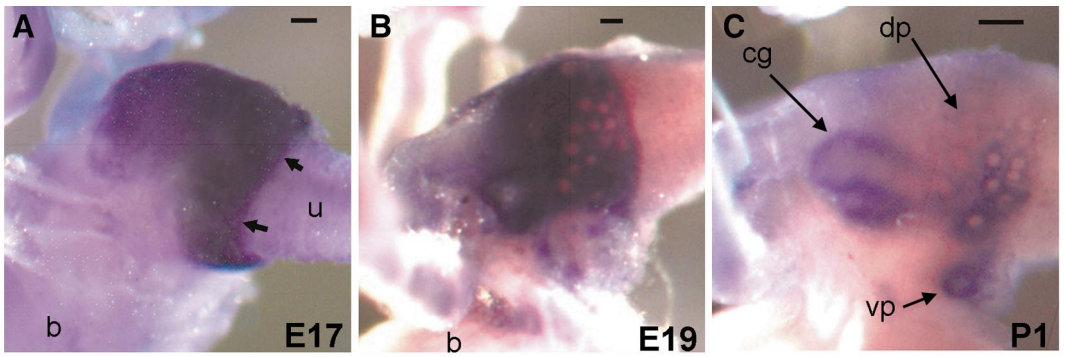

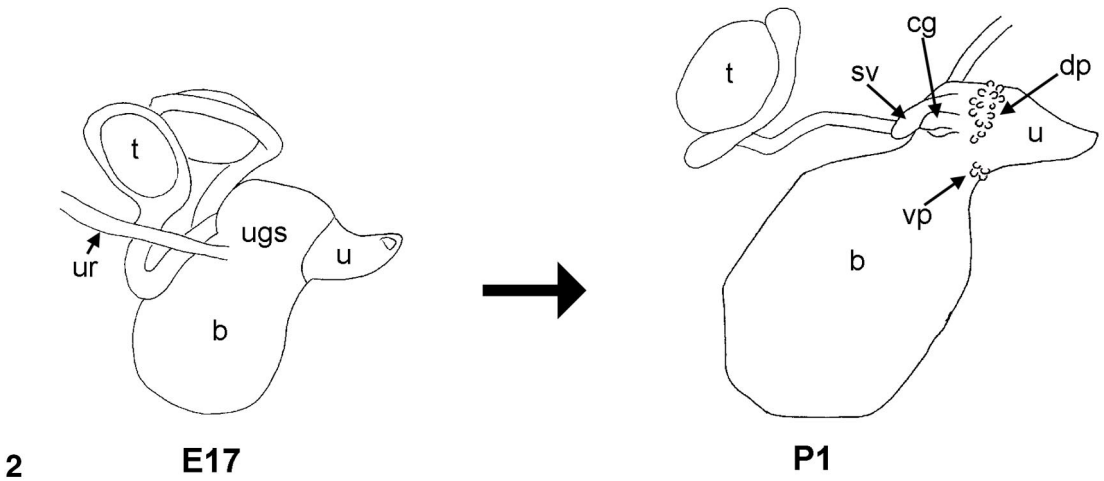

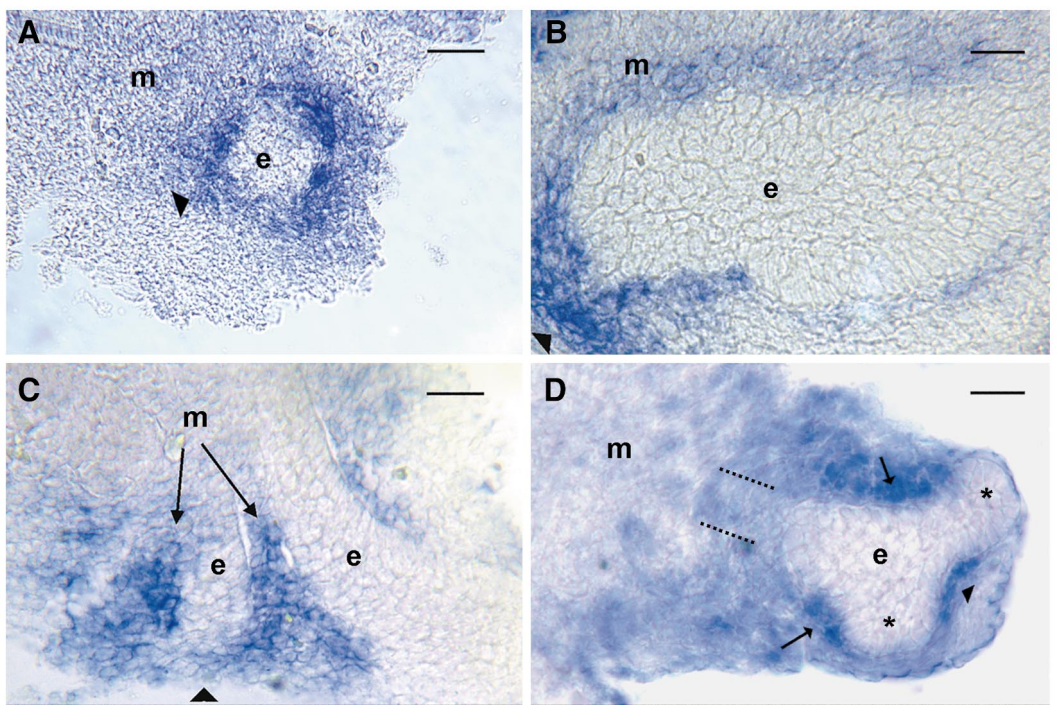

FIG. 2. Localization of *Bmp4* expression in the male urogenital sinus and developing prostate by whole-mount *in situ* hybridization. (A) A broad distribution of staining (dark purple) for *Bmp4* message in the urogenital sinus at E17 is evident. Arrows demarcate the caudal boundary of *Bmp4* expression with the adjacent urethra (u). (B) At E19, the domain of *Bmp4* expression in the urogenital sinus is punctuated

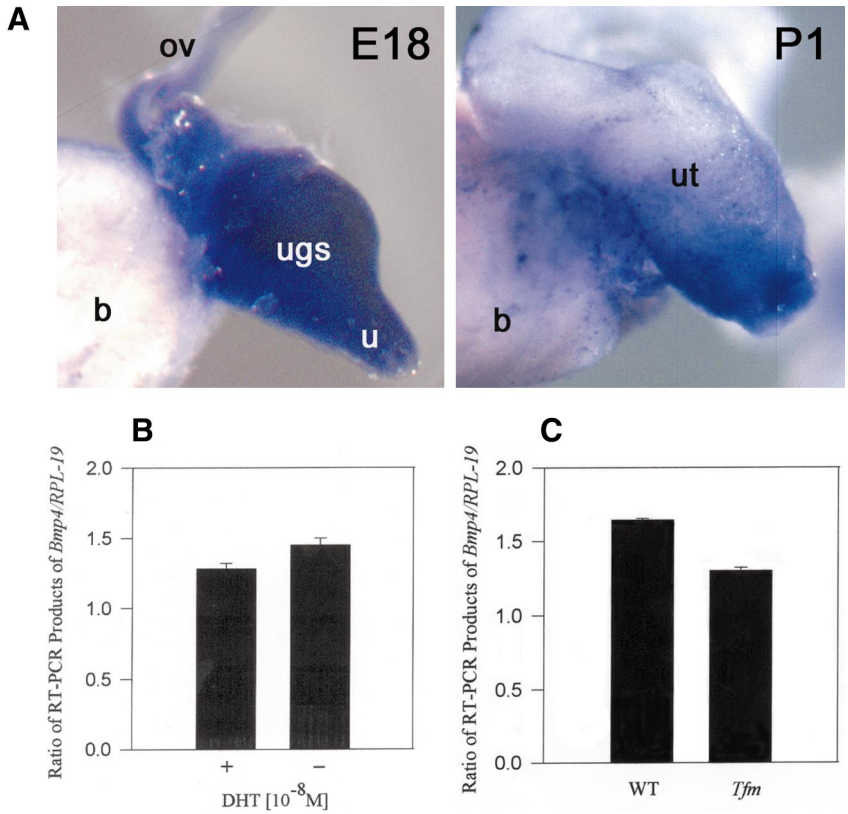

FIG. 4. *Bmp4* expression in the urogenital sinus is not androgen-dependent. (A) At E18, staining for *Bmp4* message is seen throughout the urogenital sinus (ugs) and the urethra (u) of the female lower urogenital tract. At P1, diffuse *Bmp4* expression persists in the urogenital sinus region caudal to the uterus (ut). ov, oviduct; b, bladder. (B) QRT-PCR for *Bmp4* expression in male urogenital sinus tissues obtained at E15 and cultured for 72 h in the presence or absence of 10^{-8} M DHT. Each bar represents the mean ± SEM of triplicate assays of RNA from pooled samples (n = 4 tissues). (C) QRT-PCR for *Bmp4* expression in urogenital sinus tissues obtained at P1 from male C57BL/6J-$A^{w\text{-}J}$-Ta^{6J}+/+Ar^{Tfm} mutant mouse with testicular feminization (*Tfm*) and its wildtype control (WT). Each bar represents the mean ± SEM of triplicate assays of RNA from individual samples. For both (B) and (C), assays were performed utilizing the message for ribosomal subunit *RPL-19* as an internal standard. Please note that higher *Bmp4/RPL-19* product ratios in these experiments compared to those of Fig. 1 were the result of using a newly synthesized set of *Bmp4* primers which yielded a higher efficiency reaction than that of the *RPL-19* standard.

---

by circular areas with little or no apparent staining for *Bmp4* message. (C) *Bmp4* expression is concentrated around the emerging prostatic main ducts at P1. Ducts of both the dorsal prostate (dp) and ventral prostate (vp) are ringed with staining for *Bmp4* message and their "punched out" appearance is evident. Staining also outlines the main ducts of the coagulating gland (cg). The sketches on the bottom panels illustrate the gross morphological changes in the male lower urogenital tract as the prostate develops from its anlage in the urogenital sinus (ugs) prior to onset of prostatic budding at E17 to the early appearance of prostatic ductal buds in the coagulating gland (cg), dorsal prostate (dp), and ventral prostate (vp) at P1. b, bladder; u, urethra; dp, dorsal prostate; vp, ventral prostate; cg, coagulating gland; t, testis; ur, ureter; ugs, urogenital sinus; sv, seminal vesicle. Scale bar = 100 μm. Data are representative of at least two animals per time point analyzed.

FIG. 3. Mesenchymal distribution of *Bmp4* expression in sections of P1 whole-mount *in situ* hybridization specimens. (A) Cross section of a prostatic duct reveals *Bmp4* expression (arrowhead) surrounding the ductal bud as suggested by "punched out" appearance of the whole-mount *in situ* specimens (see Fig. 2C). (B) *Bmp4* expression is concentrated in and restricted to the mesenchyme (m) surrounding the prostatic bud epithelium (e). (C) Staining for *Bmp4* expression is intense in mesenchyme separating prostatic buds (arrows). The staining for *Bmp4* expression in the mesenchyme around apical ends of ducts cut in longitudinal section (arrowheads) varied from strong (B) to relatively light (C). Section of a main duct (D) branching into two lateral buds (asterisks) shows *Bmp4* expression is concentrated in the periductal mesenchyme proximal to the branch point (arrows) and also in the mesnchyme separating the nascent branches (arrowhead). The axis of the duct proximal to the branch point, determined by examination of adjacent sections (not shown), is delineated by dotted lines. No apparent staining for *Bmp4* in the epithelium (e) is evident in any of the sections examined. The mesenchymal and epithelial designations were confirmed by immunostaining for the mesenchyme-specific marker vimentin (not shown). Scale bar = 20 μm for (A)–(C); 10 μm for (D).

the developing prostate, but the expression is relatively low (Fig. 1, inset). QRT-PCR analysis of the time course of *Bmp2* expression revealed maximal expression at E18 with comparable expression in all three prostate lobes at P5 (data not shown).

Localization of *Bmp4* message by whole-mount *in situ* hybridization revealed a changing distribution of *Bmp4* expression in the developing prostate. *Bmp4* message was initially localized to a broad and apparently uniform expression domain encompassing the prostatic anlage of the male urogenital sinus at E15 (data not shown) and E17 (Fig. 2A). A clear inferior boundary of *Bmp4* expression corresponded to the caudal margin of the prostatic anlage and demarcated the junction with the adjacent urethra (Fig. 2A, denoted with arrows). The specificity of staining for *Bmp4* expression was evidenced by lack of staining when a sense probe for *Bmp4* was used (data not shown). Later in development (E19), the homogeneous distribution of *Bmp4* expression in the urogenital sinus was punctuated by circular areas with a "punched out" appearance that seemed to reflect little or no staining for *Bmp4* message. These "punched out" circles appeared only in the region of the urogenital sinus where ductal budding occurs (Fig. 2B). As prostatic main buds appeared in distinct clusters forming the dorsal prostate, ventral prostate, and coagulating gland at P1, *Bmp4* expression was cleared from most of the urogenital sinus but remained highly concentrated around the nascent ducts (Fig. 2C). Staining for *Bmp4* expression at P5 outlined the developing main ducts and branches of the coagulating gland, dorsal prostate, and ventral prostate (data not shown).

Sectioning of P1 whole-mount specimens showed that *Bmp4* expression was most abundant in the mesenchyme immediately surrounding the epithelial buds (Figs. 3A–3D). Expression was localized very strongly in the mesenchyme separating adjacent buds (Fig. 3C). Sections of a main duct branching into two lateral buds (Fig. 3D) revealed concentrated staining for *Bmp4* expression in the periductal mesenchyme proximal to the branch point (arrows) and in the mesenchyme separating the two nascent branches (arrowhead). No epithelial staining for *Bmp4* expression was observed at any of the time points analyzed. This finding is in agreement with our previous demonstration by RT-PCR that *Bmp4* expression in the E16 male urogenital sinus is confined strictly to the mesenchyme (Podlasek *et al.*, 1999c).

Bmp4 Expression Is Not Androgen-Dependent

Because prostate development is unique to the male, we examined whether *Bmp4* expression was dependent on testosterone. Whole-mount *in situ* hybridization of E18 female lower urogenital tract revealed a wide domain of *Bmp4* expression in the urogenital sinus (Fig. 4A) comparable to that in the E17 male (Fig. 2A). At P1, however, *Bmp4* expression remained diffusely distributed in the urogenital sinus region caudal to the uterus without the "punched out" areas evident in the P1 male (compare Fig. 4A, P1 with Fig. 2C). To test directly the androgen dependence of *Bmp4* expression, male urogenital sinus tissues were obtained at E15 and cultured for 72 h in the presence or absence of 10^{-8} M dihydrotestosterone (DHT). QRT-PCR analysis showed comparable levels of *Bmp4* expression (Fig. 4B). Similarly, no significant difference in level of expression was observed when tissues were harvested at E18 and cultured for 72 h in the presence or absence of DHT (data not shown). Because testosterone secretion in the male begins prior to E15 (Cunha, 1973), we considered the possibility that earlier exposure to androgen might program *Bmp4* expression in the prostatic anlage. To address this issue, we compared *Bmp4* expression in male mice with mutant androgen receptors (testicular feminization: *Tfm*) and their wildtype controls. The *Tfm* is a frameshift mutation of the androgen receptor that renders the males insensitive to androgens (Charest *et al.*, 1991). Assay for *Bmp4* expression by QRT-PCR in the P1 urogenital sinus of *Tfm* mice and their wildtype controls (i.e., same strain background as that of *Tfm* mice) showed minimal difference in expression (Fig. 4C). These data indicate that *Bmp4* expression in the developing prostate is not testosterone-dependent.

BMP4 Inhibits Prostate Epithelial Proliferation

The biological effect of BMP4 is mediated by binding to a membrane-bound heterodimer receptor composed of a BMP type II receptor (BMPR-II) complexed with either of two type I receptors, BMPR-IA or BMPR-IB (Yamashita *et al.*, 1996). To determine which of the ligand-binding type I receptors were expressed in the developing prostate, semiquantitative RT-PCR on RNA from separated epithelium and mesenchyme of E16 urogenital sinus was performed using primers specific to *BMPR-IA* and *BMPR-IB*. We previously used this technique of tissue separation to demonstrate the specificity of *Shh* and *Bmp4* expression in the epithelium and mesenchyme, respectively (Podlasek *et al.*, 1999a,c). As shown in Fig. 5, both *BMPR-IA* (lane 1) and *BMPR-IB* (lane 2) were expressed in the separated urogenital sinus mesenchyme (UGM). Control reactions performed with primers for the mesenchymal marker *Bmp4* (lane 3) and the epithelial marker *Shh* (lane 4) confirmed the purity of the mesenchymal sample. Expression of *BMPR-IA* (lane 5) and *BMPR-IB* (lane 6) was also detected in the separated urogenital sinus epithelium (UGE). When control reactions were performed with primers for *Bmp4* (lane 7) and *Shh* (lane 8) to check the purity of the epithelial preparation, a faint *Bmp4* product band was observed. Identical results were obtained with three different preparations of separated epithelium. This could reflect either low-level *Bmp4* expression in the epithelium or slight mesenchymal contamination of the epithelial preparation. In either case, the *Bmp4* product band is extremely faint. The *BMPR-IA* and *BMPR-IB* product bands are strong by contrast and are consistent with expression of both receptors in the UGE.

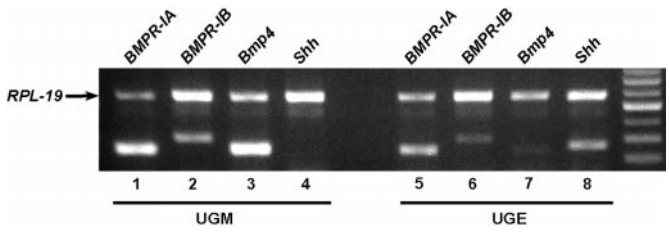

FIG. 5. Semiquantitative RT-PCR for expression of *BMP type I* receptors in separated E16 urogenital mesenchyme (UGM) and urogenital epithelium (UGE). Assay was performed on RNA from pooled tissues (n = 5–6 tissues) using primers for both *RPL-19* (as internal standard; denoted with arrow) and either *BMPR-IA* (lanes 1 and 5: 233 bp), *BMPR-IB* (lanes 2 and 6: 292 bp), *Bmp4* (lanes 3 and 7: 235 bp), or *Shh* (lanes 4 and 8: 260 bp). *BMPR-IA* and *BMPR-IB* message are expressed in both UGM and UGE. *Bmp4* and *Shh* messages were assayed to determine quality of epithelial–mesenchymal separation. Faint *Bmp4* product band in lane 7 suggests slight mesenchymal contamination of the UGE. Reactions performed in parallel without reverse transcriptase demonstrated the RNA dependence of the reaction products (data not shown).

To determine the effect of BMP4 on cell proliferation in the developing prostate, we examined the effect of exogenous BMP4 on epithelial and mesenchymal proliferation in urogenital sinus cultured *in vitro*. Affi-Gel beads soaked in either BMP4 (37.5 μg/ml in PBS) or PBS alone were implanted onto the prostatic anlagen of E17 urogenital sinus. Following 48 h of culture in serum-free, DHT-supplemented media (conditions sufficient to support ductal branching in the developing prostate; see below), BrdU incorporation in BMP4-treated and control tissues was quantitated by examining representative sections under $\times$40 magnification with the bead in the center of the field. Stained epithelial and mesenchymal cells within the area of one high-power field surrounding the bead (1.4 mm^2) were counted and BrdU-labeling indices (number of stained nuclei/total number of nuclei counted = % labeled) were determined. Control sections revealed a labeling index of 8.5% and 2.9% in the epithelium and mesenchyme, respectively (Table 1). BMP4 treatment significantly decreased the labeling index in the epithelium from 8.5% to 2.8% ($P <$ 0.0001) without affecting that in the mesenchyme (Table 1). These data indicate a selective inhibitory effect of BMP4 on epithelial proliferation in the developing prostate.

BMP4 has been shown to induce apoptosis in several tissues (Graham *et al.*, 1994; Ganan *et al.*, 1996; Bellusci *et al.*, 1996; Jernvall *et al.*, 1998; Raatikainen-Ahokas *et al.*, 2000). To determine whether apoptosis contributed to the reduced epithelial cell proliferation index in BMP4-treated tissues, sections adjacent to those used for BrdU studies were analyzed by the TUNEL technique. Staining of control sections revealed an extremely low incidence of TUNEL-labeled cells in both the epithelial and mesenchymal compartments. Comparison of TUNEL staining in sections of BMP4-treated and control tissues did not suggest any increase in TUNEL staining in the vicinity of the BMP4-soaked beads (data not shown). Sections of prostate from an adult animal 3 days postcastration stained in parallel showed abundant TUNEL staining, verifying the sensitivity of the assay (data not shown). These observations suggest that exogenous BMP4 at the concentrations used does not cause apoptosis in either the mesenchyme or epithelium of the developing prostate.

BMP4 Inhibits Prostate Ductal Budding

BMP4 has been identified as a regulator of branching morphogenesis in the developing lung and kidney (Bellusci *et al.*, 1996; Raatikainen-Ahokas *et al.*, 2000; Miyazaki *et al.*, 2000). To determine whether BMP4 influenced prostate ductal budding, E15 male urogenital sinus tissues were maintained in serum-free, DHT-supplemented media in the absence or presence of exogenous BMP4 (30 or 300 ng/ml). Following 6 days of culture, all control prostate rudiments had grown in size and displayed extensive prostate ductal budding (compare Figs. 6A and 6B). The prostatic buds extended from the cranial region of the urogenital sinus in a bilaterally symmetrical pattern, forming an arborlike canopy with the urethra extending caudally (Fig. 6B). The ducts were mostly elongate with slightly dilated apical ends and the beginnings of ductal branching can be discerned (Fig. 6B, denoted with arrow).

Among tissues treated with exogenous BMP4, the number and/or size of ductal buds were decreased (Figs. 6C and 6D). The effect was more pronounced at the higher concentration of BMP4 used (300 ng/ml) where eight out of 12 (67%) prostate rudiments exhibited either barely discernible, stumplike outgrowths (not shown) or just a few prostatic buds (Fig. 6D). To quantitate morphological differences, the number of discernible ductal tips was counted from photographs of individual prostate rudiments taken at the same magnification. BMP4 significantly reduced the mean number of prostate ductal tips in a dose-dependent manner (Fig. 6E).

TABLE 1
Effect of BMP4 on Cellular Proliferation

	Stained/total nuclei (labeling index)		
Tissue layer	Control beads	BMP4 beads	*P*
Epithelium	630/7435 (8.5%)	229/8193 (2.8%)*	<0.0001
Mesenchyme	542/18,860 (2.9%)	481/18,091 (2.7%)	0.21

Note. Affi-Gel beads soaked in either PBS (Control) or BMP4 (37.5 μg/ml) were implanted onto E17 male urogenital sinus tissues. Following 48 h of culture, BrdU staining of tissues was performed and the labeling index was determined.

*$P <$ 0.0001 between control and BMP4-treated epithelial labeling indices determined from 11 control and 10 BMP4-treated urogenital sinus tissues.

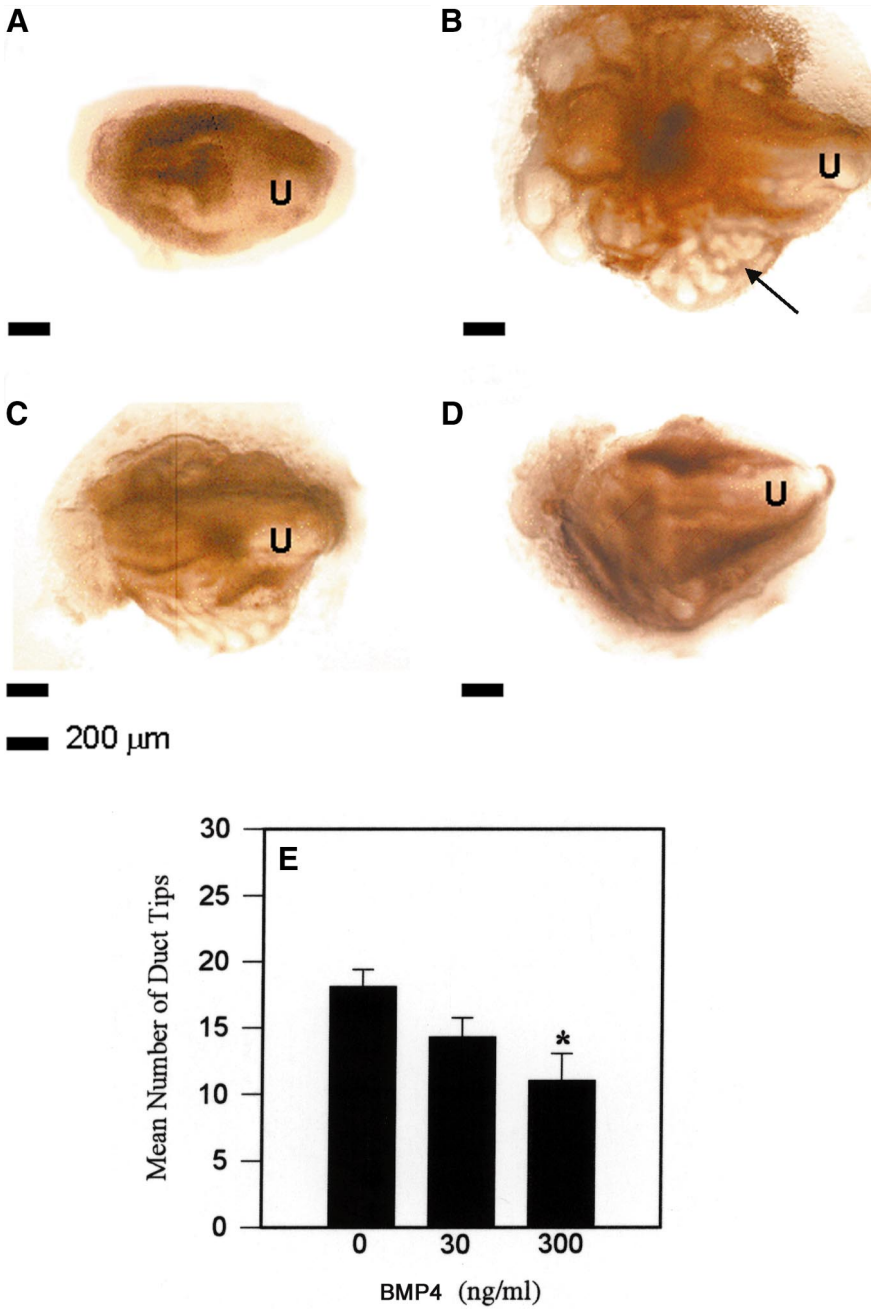

FIG. 6. Exogenous BMP4 inhibits prostate ductal budding. Male urogenital sinus tissues obtained at E15 (A) were cultured for 6 days in serum-free, testosterone-supplemented medium in the absence (B) or presence (C, D) of BMP4. (B) The control prostate rudiments had grown in size and developed numerous buds in the urogenital sinus. Ductal branching is evident (arrow). In the presence of BMP4 at either 30 (C) or 300 ng/ml (D), prostate rudiments exhibited fewer prostatic buds than those of controls (B). (E) Quantitative analysis of budding showed that BMP4 at 300 ng/ml significantly (*$P = 0.008$) reduced the mean number of ductal tips. Each bar represents the mean (± SEM) of 11–12 prostatic tissues per treatment group. Scale bar = 200 μm. u, urethra.

Effect of Bmp4 Haploinsufficiency

To investigate the normal role of BMP4 in prostate development, we examined the effect of *Bmp4* partial loss of function. Homozygous *Bmp4* loss-of-function mutation in the mouse is lethal between E6.5 and E9.5 (Winnier *et al.*, 1995), a period prior to initiation of prostate development.

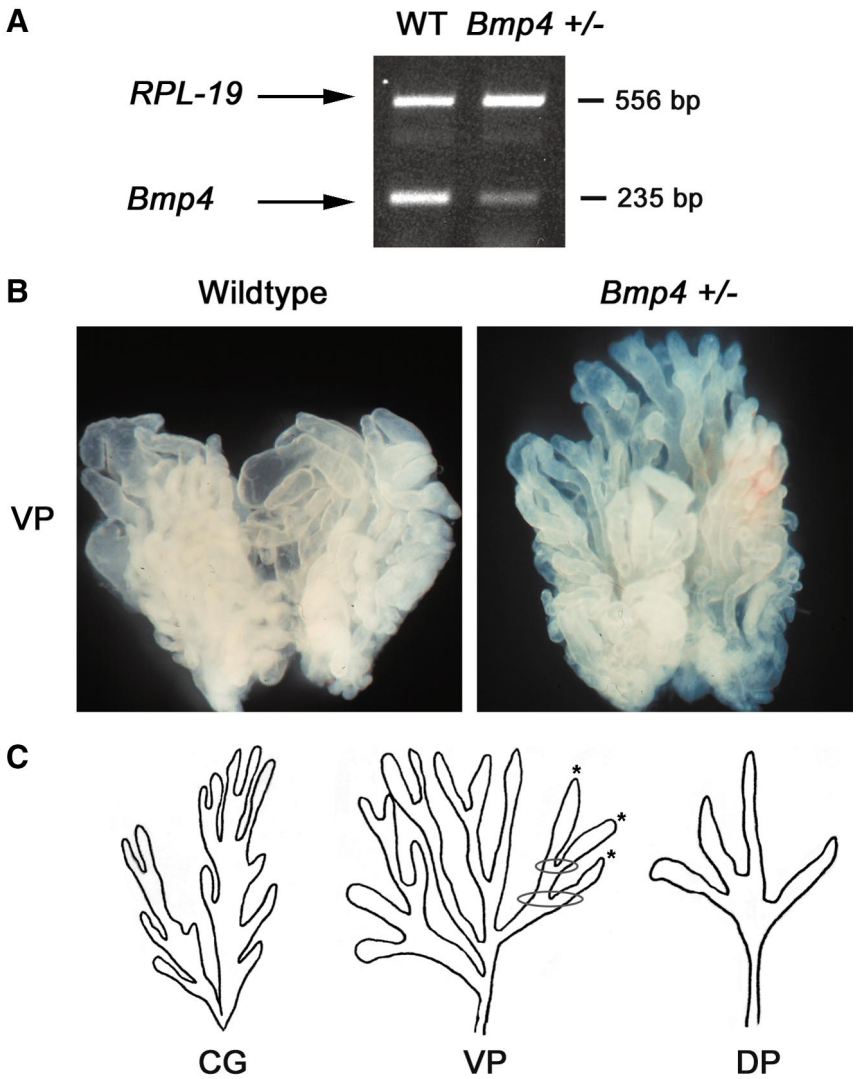

FIG. 7. Effect of *Bmp4* haploinsufficiency. (A) Semiquantitative RT-PCR for *Bmp4* expression in prostate of P1 $Bmp4^{tm1Blh}$ haploinsufficient (*Bmp4* +/−) and its wildtype control (WT) was performed on RNA from individual samples. Comparison of *Bmp4* (235 bp) and *RPL19* (556 bp) product band intensities suggests that *Bmp4* expression is lower in the haploinsufficient mouse. (B) Ventral prostate lobes (VP) from adult wildtype and transgenic *Bmp4* +/− mice exhibit no major gross morphological differences. (C) Schematic illustration of ductal architecture in the adult coagulating gland (CG), ventral prostate (VP), and dorsal prostate (DP). In the schematic for VP, two branch points (encircled) and three duct tips (*) are marked to illustrate how these ductal morphologic features are quantitated.

However, the heterozygous mutants (haploinsufficient) are viable (Dunn *et al.*, 1997). We first confirmed by RT-PCR analysis that the level of *Bmp4* expression in the developing prostate of mutant *Bmp4* haploinsufficient mice was lower than that in wildtype animals (Fig. 7A). The effect of *Bmp4* partial loss of function on prostate ductal development was then determined through quantitative morphologic comparison of prostate size and ductal architecture between adult *Bmp4* haploinsufficient animals and their wildtype controls. No gross morphological differences were consistently observed among the different prostate lobes, as illustrated by a comparison of the wildtype and mutant ventral prostate (Fig. 7B). To determine whether *Bmp4* haploinsufficiency would alter the number of ductal buds that develop into main prostatic ducts, we compared the number of main ducts in the coagulating gland, ventral prostate, and dorsal prostate of adult mutant and wildtype mice. No significant differences were observed (Table 2A). However, quantitative analysis of the ductal architecture in the haploinsufficient mice did reveal significant increases in the number of duct tips in the coagulating gland and ventral prostate (Table 2B).

TABLE 2

A. Comparison of number of main ducts in prostate lobes of adult wildtype and heterozygous *Bmp4* mutant mice.

Prostate lobe	Number of main ducts	
	Wildtype	*Bmp4* mutant
Coagulating gland	4 (±0)	4 (±0)
Ventral prostate	6 (±0.5)	4 (±0.5)
Dorsal prostate	18 (±2)	19 (±3)

B. Quantitative morphologic analysis of ductal branching in prostate lobes of adult wildtype and heterozygous *Bmp4* mice.

Prostate lobe	Wet weight (mg)		Number of branch points		Number of duct tips	
	Wildtype	*Bmp4* mutant	Wildtype	*Bmp4* mutant	Wildtype	*Bmp4* mutant
Coagulating gland	25.8 (±1.2)	29.8 (±2.6)	30 (±3)	36 (±6)	140 (±4)	172 (±11)*
Ventral prostate	13.2 (±1.1)	11.0 (±1.9)	58 (±4)	73 (±5)*	131 (±4)	164 (±11)*
Dorsal prostate	16.6 (±1.1)	13.5 (±1.5)	102 (±8)	107 (±8)	240 (±6)	247 (±10)

Note. Values are means ± SEM.
*$P < 0.05$.

The ductal architecture of prostatic lobes can be comprehensively examined by isolating the individual lobes and microdissecting the tissues to expose the complete ductal network. The number of duct tips and branch points provide a reproducible and quantitative measure of ductal morphogenesis that can be used to assay the effect of genetic and chemical dysregulation on ductal morphogenesis (Seo *et al.,* 1997; Podlasek *et al.,* 1997, 1999a,b). The three prostate lobes display distinct ductal architectures (Lung and Cunha, 1981; Sugimura *et al.,* 1986) as illustrated in Fig. 7C. Each coagulating gland lobe consists of two main ducts with multiple secondary and rare tertiary branches (Fig. 7C) (Lung and Cunha, 1981). We observed a statistically significant 23% increase in the mean number of duct tips in the coagulating glands of *Bmp4* haploinsufficient mice (Table 2B). Our analysis also showed an increase in the mean number of branch points in the coagulating gland of *Bmp4* haploinsufficient mice, although the difference did not reach statistical significance. In that we did not observe any additional main ducts in the coagulating glands of the mutant mice, the increase in duct tips can be attributed to an increased number of branching events. Each ventral prostate lobe consists of 1–3 main ducts that undergo a dichotomous pattern of branching (Fig. 7C) (Sugimura *et al.,* 1986). We observed a statistically significant increase in both the mean number of duct tips and branch points in the ventral prostate of the mutants (Table 2B). Each dorsal prostate lobe consists of multiple main ducts that branch distally into several ducts (Fig. 7C) (Sugimura *et al.,* 1986). Our analysis revealed a slight increase in the mean number of duct tips and branch points in the dorsal prostate of the mutant animals, although the differences were not statistically significant (Table 2B). To complete the analysis of the prostate in the haploinsufficient animals, histologic sections of the adult mutant and wildtype animals were examined in blinded fashion. This revealed no obvious differences in epithelial or stromal differentiation (data not shown).

DISCUSSION

Prostatic ductal budding and branching is postulated to result from regulated cross-talk involving stimulatory and inhibitory signaling and transcription factors in both the mesenchyme and epithelium. The known factors that influence prostate ductal morphogenesis are shown in Fig. 8. We provide evidence that BMP4 is a mesenchymal factor that restricts prostatic ductal budding and branching by inhibiting epithelial cell proliferation. To demonstrate this effect, we utilized *in vitro* culture of E15 male mouse prostate rudiments in testosterone-supplemented media to mimic the *in vivo* process of prostatic budding. This 6-day *in vitro* culture corresponds to the time span E15-P1 *in vivo,* a period when the coagulating gland main ducts, ventral prostate main ducts, and some of the dorsal prostate main ducts are formed (Lung and Cunha, 1981; Sugimura *et al.,* 1986). In this culture system, exogenous BMP4 inhibited prostatic ductal budding in a dose-dependent fashion. Companion studies revealed a specific inhibitory effect of BMP4 on epithelial cellular proliferation.

An inhibitory effect of BMP4 on bud formation and ductal branching has been demonstrated in other systems. Exogenous BMP4 suppressed embryonic chick feather bud formation (Jung *et al.,* 1998) and decreased the number of ureteric tips in mouse kidney rudiments (Raatikainen-Ahokas *et al.,* 2000). Ectopic misexpression of *Bmp4* decreased the number of terminal buds and inhibited epithe-

lial proliferation in transgenic embryonic lung (Bellusci *et al.,* 1996). Similarly, misexpression of *Bmp4* inhibited cellular proliferation and disrupted hair follicle morphogenesis in transgenic mice (Blessing *et al.*, 1993). Our localization studies paint a dynamic pattern of *Bmp4* expression in the developing prostate. Prior to any morphological evidence of budding (E17), *Bmp4* is expressed widely in the urogenital sinus. Later in development, the homogeneous expression of *Bmp4* in the urogenital sinus is punctuated by circular areas that appear to express little or no *Bmp4*. These "punched out" areas coincide with the region where prostatic ducts form and it is tempting to speculate that these are sites of imminent bud formation. Eventually, *Bmp4* expression is restricted to a narrow region of mesenchyme immediately surrounding nascent epithelial buds and ductal branches. Our finding that exogenous BMP4 inhibits ductal budding suggests that clearing of *Bmp4* expression from sites of imminent bud formation relieves the restrictive action of BMP4 on epithelial proliferation and is a necessary step in bud formation.

The *Bmp4* haploinsufficient mutant mouse provided an opportunity to determine how prostate development is altered by partial loss of endogenous BMP4 function. Given the inhibitory effect of exogenous BMP4 on prostate ductal budding (present data) and the preaxial polydactyly of the hind limb in *Bmp4* heterozygous null mutants (Dunn *et al.,* 1997), we postulated that *Bmp4* haploinsufficiency might increase prostate size, ductal budding, and/or ductal branching. Our analysis revealed no increase in overall prostate size and no gross morphological changes. There was no increase in the number of main prostatic ducts in the coagulating gland, dorsal prostate, or ventral prostate. This finding indicates that the number of ductal buds is not increased by *Bmp4* haploinsufficiency and suggests that diminished *Bmp4* expression is not sufficient to initiate main duct formation. A critical role for other factors in determining the sites of ductal budding is consistent with our previous finding that the number of main prostatic ducts is reduced by mutations in the *Hox* genes *Hoxd-13* and *Hoxa-13* (Podlasek *et al.,* 1997, 1999b). On the other hand, *Bmp4* haploinsufficiency does produce an increase in ductal branching in both the coagulating gland and ventral prostate, a result suggesting that *Bmp4* plays an active role in determining the number of branching events during ductal morphogenesis. The distribution of *Bmp4* expression in the periductal mesenchyme and its apparent diminished expression at nascent branch points (Fig. 3D) suggest that BMP4 may serve to actively restrict branching and that *Bmp4* haploinsufficiency compromises this function.

The *Bmp4* partial loss of function mutation affected branching morphogenesis in the ventral prostate and coagulating gland more than in the dorsal prostate. The period of high *Bmp4* expression, E14 through P1, embraces a time when ventral prostate main ducts form and begin to branch (Sugimura *et al.*, 1986). The main ducts of the coagulating gland also form by P1 and ductal branches appear at P3 (Lung and Cunha, 1981). This is in contrast to the dorsal prostate, in which main duct formation begins prenatally but ductal branching does not occur intensively until P10 (Sugimura *et al.,* 1986), a period when *Bmp4* expression is already on the decline. The offset in timing of ductal branching in the different prostate lobes may be indicative of different molecular mechanisms that control branching. Such prostate lobe-specific effects have been observed previously: retinoic acid administration to newborn mice inhibited branching in the ventral prostate more severely than in the dorsal prostate (Seo *et al.,* 1997). An alternate explanation for the differential effect of *Bmp4* loss-of-function mutation on branching in the ventral prostate and dorsal prostate would be a ventral–dorsal axis of differential sensitivity to endogenous BMP4 action. In the developing kidney, an anterior–posterior axis of BMP4 responsiveness has been postulated to explain the severity of branching deformities in the anterior versus the posterior half of the ureteric bud in response to exogenous BMP4 (Raatikainen-Ahokas *et al.,* 2000).

Bmp4 has been postulated to regulate branching in the developing lung and kidney (Bellusci *et al.,* 1996; Raatikainen-Ahokas *et al.,* 2000; Miyazaki *et al.,* 2000), determine the spacing of developing teeth (Vainio *et al.,* 1993; Neubuser et al.,1997), and control the spacing of feather primordia in chick epidermis (Jung *et al.,* 1998; Noramly and Morgan, 1998). The basic model for development in these systems postulates that budding is determined by an interaction of positive growth regulators (e.g., members of the FGF family and Shh) and negative growth regulators (such as BMP4 and/or BMP2) (Jung *et al.,* 1998; Hogan, 1999). According to this model, the negative regulator modulates the response to the positive growth signal so as to determine a discrete site of bud formation while providing lateral inhibition to create spacing between buds. In these other systems, *Bmp4* expression is essentially uniform over the region of the developing bud. Formation of a bud in the center of the *Bmp4* expression domain but inhibition in the lateral domain is postulated to result from differing balances of positive and negative growth signaling that accrue from different diffusional properties of positive and negative signaling molecules (Jung *et al.*, 1998; Hogan, 1999).

The developing prostate appears to be different in two respects. First, our studies show that *Bmp4* expression is cleared at the site of bud formation and this may provide a focal release of growth inhibition at the apical zone to allow for proximal–distal elongation. Second, the failure of *Bmp4* haploinsuffiency to produce an increase in the number of main ducts suggests that *Bmp4* expression does not directly determine the number and spacing of budding events. As buds elongate, *Bmp4* expression outlines the mesenchyme along the axis of growing ducts (see Fig. 2C). Having found that genetic haploinsufficiency for *Bmp4* produced an increase in ductal branching in the coagulating gland and ventral prostate, we postulate that the canonical pattern of *Bmp4* expression in elongating ducts normally serves to restrict lateral branching.

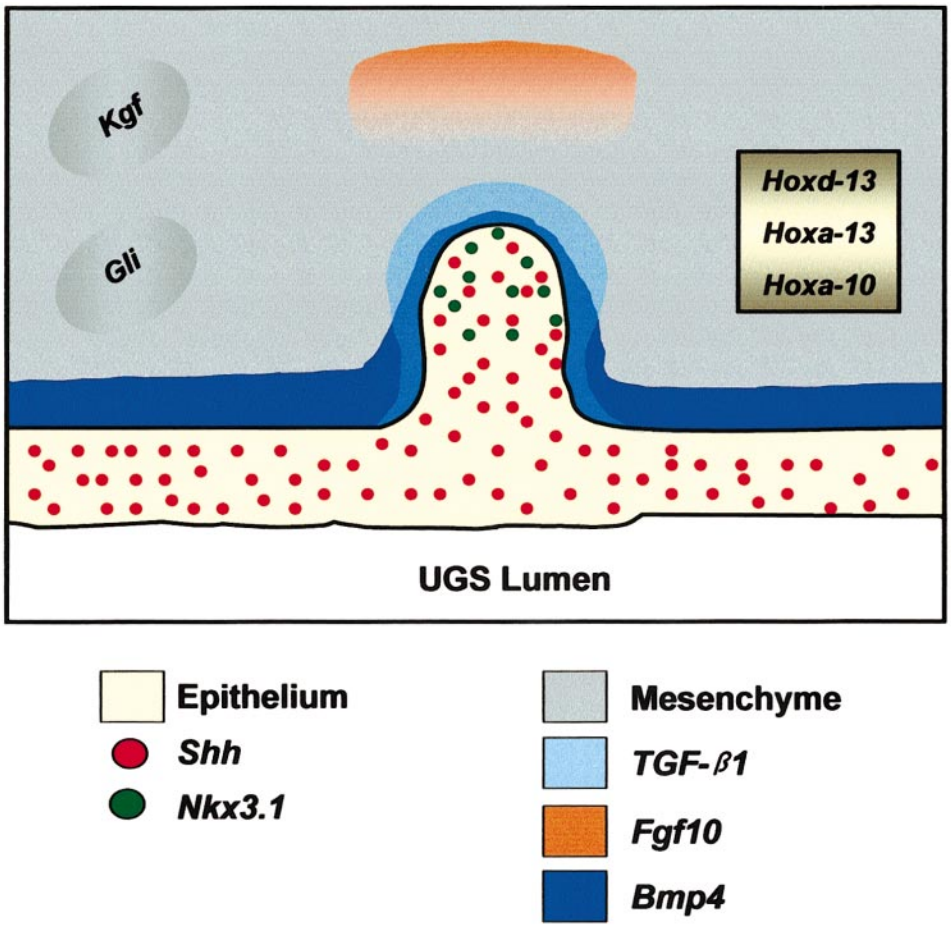

FIG. 8. Factors that regulate ductal budding and branching morphogenesis in the developing prostate. *Bmp4* expression in the mesenchyme is strongest immediately surrounding the prostatic buds and is weaker at the apical tip. *TGF-β1* is expressed predominantly in the urogenital sinus mesenchyme and TGF-β1 protein has been localized to mesenchyme surrounding emerging prostatic ducts (Timme *et al.*, 1994). Mice with mutation in *TGF-β1* were previously reported to exhibit defects in prostate duct formation (cited in Abate-Shen and Shen, 2000). *Fgf10* is expressed in the urogenital sinus mesenchyme peripheral to the periurethral mesenchyme and distal to the elongating prostatic ducts. FGF10 stimulates the development of ventral prostate explants in an *in vitro* organ culture (Thomson and Cunha, 1999). *Kgf* is expressed in the urogenital sinus mesenchyme, although its exact localization in relation to the prostatic ducts is not yet known (Finch *et al.*, 1995). KGF stimulates ductal branching in the absence of testosterone (Sugimura *et al.*, 1996; Thomson *et al.*, 1997). *Shh* is expressed in the urogenital sinus epithelium during the period of ductal budding and antibody blockade of Shh function abrogates prostate ductal morphogenesis (Podlasek *et al.*, 1999a). The transcription factor *Gli*, a conserved target of Shh signaling, is expressed in the mesenchyme and expression is upregulated by Shh (Podlasek *et al.*, 1999a; manuscript in preparation). *Nkx3.1*, a member of the murine *Nkx* homeobox gene family, is expressed in the urogenital sinus epithelium and expression is localized to the distal edges of emerging prostatic epithelial buds (Sciavolino *et al.*, 1997). Homozygous mutant mice for *Nkx3.1* exhibit prostatic epithelial hyperplasia and defective branching morphogenesis (Bhatia-Gaur *et al.*, 1999; Tanaka *et al.*, 2000). *Hoxd-13*, *Hoxa-13*, and *Hoxa-10* are expressed in both the epithelial and mesenchymal compartments of the male urogenital sinus (Oefelein *et al.*, 1996; Podlasek *et al.*, 1999b,c). Phenotypic analysis of mice with mutations in these *Hox* genes revealed multiple abnormalities in male accessory sex organs including diminished main duct formation in the coagulating gland (*Hoxa-13*) and dorsal prostate (*Hoxd-13*) and diminished ductal branching in the coagulating gland (*Hoxa-10*), dorsal prostate (*Hoxd-13* and *Hoxa-13*), and ventral prostate (*Hoxa-13*) (Podlasek *et al.*, 1997, 1999b,c). More severe abnormalities of prostate development are evident with compound *Hoxa-13* and *Hoxd-13* mutations (Warot *et al.*, 1997).

We previously demonstrated the expression of *sonic hedgehog* (*Shh*) in the urogenital sinus epithelium and showed that antibody blockade of Shh function abrogates prostate growth and glandular development (Podlasek *et al.*, 1999a). The localization of *Shh* expression to the urogenital epithelium of embryonic prostate (Podlasek *et al.*, 1999a) and of *Bmp4* expression to the surrounding mesenchyme (present study) mirrors the *Shh-Bmp4* pattern of expression

at other sites of mesenchymal–epithelial interaction in the developing embryo. While this colocalization has led to speculations that *Bmp4* is a downstream target of Shh signaling (Bitgood and McMahon, 1995), *Bmp4* expression was maintained in the developmentally arrested hair follicles of $Shh^{-/-}$ mutant mouse embryos (St-Jacques *et al.*, 1998). Our own (unpublished) observations seem to indicate that *Bmp4* is not a direct downstream target gene of Shh signaling because antibody blockade of Shh signaling does not abolish *Bmp4* expression in the developing mouse prostate. However, this does not preclude an interaction between BMP4 and Shh signaling pathways in the regulation of prostate development.

ACKNOWLEDGMENTS

We thank Dr. Brigid Hogan (Vanderbilt University Medical Center, Nashville, TN) for the generous gift of *Bmp4* cDNA plasmid. We also thank Genetics Institute, Inc. (Cambridge, MA) for the generous supply of recombinant human BMP4 protein and the BMP4 antibody. This work was supported by grants from the National Institutes of Health (DK 02426, DK 52687) and the National Institute of Environmental Health Sciences (PO1 ES10549).

REFERENCES

Abate-Shen, C., and Shen, M. M. (2000). Molecular genetics of prostate cancer. *Genes Dev.* **14,** 2410–2434.

Bellusci, S., Henderson, R., Winnier, G., Oikawa, T., and Hogan, B. L. M. (1996). Evidence from normal expression and targeted misexpression that *Bone Morphogenetic Protein-4* (*Bmp-4*) plays a role in mouse embryonic lung morphogenesis. *Development* **122,** 1693–1702.

Bhatia-Gaur, R., Donjacour, A. A., Sciavolino, P. J., Kim, M., Desai, N., Young, P., Norton, C. R., Gridley, T., Cardiff, R. D., Cunha, G. R., Abate-Shen, C., and Shen, M. M. (1999). Roles for *Nkx3.1* in prostate development and cancer. *Genes Dev.* **13,** 966–977.

Bitgood, M. J., and McMahon, A. P. (1995). *Hedgehog* and *Bmp* genes are coexpressed at many diverse sites of cell–cell interaction in the mouse embryo. *Dev. Biol.* **172,** 126–138.

Blessing, M., Nanney, L. B., King, L. E., Jones, C. M., and Hogan, B. L. M. (1993). Transgenic mice as a model to study the role of TGF-β-related molecules in hair follicles. *Genes Dev.* **7,** 204–215.

Charest, N. J., Zhou, Z., Lubahn, D. B., Olsen, K. L., Wilson, E. M., and French, F. S. (1991). A frameshift mutation destabilizes androgen receptor messenger RNA in the *Tfm* mouse. *Mol. Endocrinol.* **5,** 573–581.

Cooke, P. S., Young, P. F., and Cunha, G. R. (1987). A new model system for studying androgen-induced growth and morphogenesis *in vitro*: The bulbourethral gland. *Endocrinology* **121,** 2161–2170.

Cunha, G. R. (1973). The role of androgens in the epithelio-mesenchymal interactions involved in prostatic morphogenesis in embryonic mice. *Anat. Rec.* **175,** 87–96.

Cunha, G. R., and Donjacour, A. (1987). Mesenchymal-epithelial interactions: Technical considerations. *In* "Current Concepts and Approaches to the Study of Prostate Cancer," pp. 273–282. A. R. Liss Inc., New York.

Cunha, G. R., Donjacour, A. A., Cooke, P. S., Mee, S., Bigsby, R. M., Higgins, S. J., and Sugimura, Y. (1987). The endocrinology and developmental biology of the prostate. *Endocr. Rev.* **8,** 338–362.

Cunha, G. R., and Lung, B. (1979). Development of male accessory glands. *In* "Accessory Glands of the Male Reproductive Tract", Vol. 6, pp. 1–28. Ann Arbor Science, Ann Arbor, MI.

Dunn, N. R., Winnier, G. E., Hargett, L. K., Schrick, J. J., Fogo, A. B., and Hogan, B. L. M. (1997). Haploinsufficient phenotypes in *Bmp4* heterozygous null mice and modification by mutations in *Gli3* and *Alx4*. *Dev. Biol.* **188,** 235–247.

Finch, P. W., Cunha, G. R., Rubin, J. S., Wong, J., and Ron, D. (1995). Pattern of keratinocyte growth factor and keratinocyte growth factor receptor expression during mouse fetal development suggests a role in mediating morphogenetic mesenchymal–epithelial interactions. *Dev. Dyn.* **203,** 223–240.

Ganan, Y., Macias, D., Duterque-Coquillaud, M., Ros, M. A., and Hurle, J. M. (1996). Role of TGFβs and BMPs as signals controlling the position of the digits and the areas of interdigital cell death in the developing chick limb autopod. *Development* **122,** 2349–2357.

Gelbart, W. M. (1989). The *decapentaplegic* gene: A TGF-β homologue controlling pattern formation in *Drosophila*. *Development* **107,** *(Suppl.)*, 65–74.

Graham, A., Francis-West, P., Brickell, P., and Lumsden, A. (1994). The signalling molecule BMP4 mediates apoptosis in the rhombencephalic neural crest. *Nature* **372,** 684–686.

Guo, L., Degenstein, L., and Fuchs, E. (1996). Keratinocyte growth factor is required for hair development but not for wound healing. *Genes Dev.* **10,** 165–175.

Harris, S. E., Harris, M. A., Mahy, P., Wozney, J., Feng, J. Q., and Mundy, G. R. (1994). Expression of bone morphogenetic protein messenger RNAs by normal rat and human prostate and prostate cancer cells. *Prostate* **24,** 204–211.

Haughney, P. C., Hayward, S. W., Dahiya, R., and Cunha, G. R. (1998). Species-specific detection of growth factor gene expression in developing murine prostatic tissue. *Biol. Reprod.* **59,** 93–99.

Hogan, B. L. M. (1996). Bone morphogenetic proteins: Multifunctional regulators of vertebrate development. *Genes Dev.* **10,** 1580–1594.

Hogan, B. L. M. (1999). Morphogenesis. *Cell* **96,** 225–233.

Itoh, N., Patel, U., Cupp, A. S., and Skinner, M. K. (1998). Developmental and hormonal regulation of transforming growth factor-β1 (TGFβ1), -2, and -3 gene expression in isolated prostatic epithelial and stromal cells: Epidermal growth factor and TGFβ interactions. *Endocrinology* **139,** 1378–1388.

Jernvall, J., Aberg, T., Kettunen, P., Keranen, S., and Thesleff, I. (1998). The life history of an embryonic signaling center: BMP4 induces *p21* and is associated with apoptosis in the mouse tooth enamel knot. *Development* **125,** 161–169.

Jung, H.-S., Francis-West, P. H., Widelitz, R. B., Jiang, T.-X., Ting-Berreth, S., Tickle, C., Wolpert, L., and Chuong, C.-M. (1998). Local inhibitory action of BMPs and their relationships with activators in feather formation: Implications for periodic patterning. *Dev. Biol.* **196,** 11–23.

Kitsberg, D. I., and Leder, P. (1996). Keratinocyte growth factor induces mammary and prostatic hyperplasia and mammary adenocarcinoma in transgenic mice. *Int. J. Dev. Biol.* **40,** 941–951.

Lung, B., and Cunha, G. R. (1981). Development of seminal vesicles and coagulating glands in neonatal mice. I. The morphogenetic effects of various hormonal conditions. *Anat. Rec.* **199,** 73–88.

Martikainen, P., Kyprianou, N., and Isaacs, J. T. (1990). Effect of transforming growth factor-β1 on proliferation and death of rat prostatic cells. *Endocrinology* **127,** 2963–2968.

Miyazaki, Y., Oshima, K., Fogo, A., Hogan, B. L. M., and Ichikawa, I. (2000). Bone morphogenetic protein 4 regulates the budding site and elongation of the mouse ureter. *J. Clin. Invest.* **105,** 863–873.

Neubuser, A., Peters, H., Balling, R., and Martin, G. R. (1997). Antagonistic interactions between FGF and BMP signaling pathways: A mechanism for positioning the sites of tooth formation. *Cell* **90,** 247–255.

Noramly, S., and Morgan, B. A. (1998). BMPs mediate lateral inhibition at successive stages in feather tract development. *Development* **125,** 3775–3787.

Oefelein, M., Chin-Chance, C., and Bushman, W. (1996). Expression of the homeotic gene Hox-d13 in the developing and adult mouse prostate. *J. Urol.* **155,** 342–346.

Podlasek, C. A., Barnett, D. H., Clemens, J. Q., Bak, P. M., and Bushman, W. (1999a). Prostate development requires sonic hedgehog expressed by the urogenital sinus epithelium. *Dev. Biol.* **209,** 28–39.

Podlasek, C. A., Clemens, J. Q., and Bushman, W. (1999b). *HOXA-13* gene mutation results in abnormal seminal vesicle and prostate development. *J. Urol.* **161,** 1655–1661.

Podlasek, C. A., Duboule, D., and Bushman, W. (1997). Male accessory sex organ morphogenesis is altered by loss of function of Hoxd-13. *Dev. Dyn.* **208,** 454–465.

Podlasek, C. A., Seo, R. M., Clemens, J. Q., Ma, L., Maas, R. L., and Bushman, W. (1999c). *Hoxa-10* deficient male mice exhibit abnormal development of the accessory sex organs. *Dev. Dyn.* **214,** 1–12.

Raatikainen-Ahokas, A., Hytonen, M., Tenhunen, A., Sainio, K., and Sariola, H. (2000). BMP-4 affects the differentiation of metanephric mesenchyme and reveals an early anterior-posterior axis of the embryonic kidney. *Dev. Dyn.* **217,** 146–158.

Sandgren, E. P., Luetteke, N. C., Palmiter, R. D., Brinster, R. L., and Lee, D. C. (1990). Overexpression of TGFα in transgenic mice: Induction of epithelial hyperplasia, pancreatic metaplasia, and carcinoma of the breast. *Cell* **61** 1121–1135.

Sciavolino, P. J., Abrams, E. W., Yang, L., Austenberg, L. P., Shen, M. M., and Abate-Shen, C. (1997). Tissue-specific expression of murine *Nkx3.1* in the male urogenital system. *Dev. Dyn.* **209,** 127–138.

Seo, R., McGuire, M., Chung, M., and Bushman, W. (1997). Inhibition of prostate ductal morphogenesis by retinoic acid. *J. Urol.* **158,** 931–935.

St-Jacques, B., Dassule, H. R., Karavanova, I., Botchkarev, V. A., Li, J., Danielian, P. S., McMahon, J. A., Lewis, P. M., Paus, R., and McMahon A. P. (1998). Sonic hedgehog signaling is essential for hair development. *Curr. Biol.* **8,** 1058–1068.

Sugimura, Y., Cunha, G. R., and Donjacour, A. A. (1986). Morphogenesis of ductal networks in the mouse prostate. *Biol. Reprod.* **34,** 961–971.

Sugimura, Y., Foster, B. A., Hom, Y. K., Lipschutz, J. H., Rubin, J. S., Finch, P. W., Aaronson, S. A., Hayashi, N., Kawamura, J., and Cunha, G. R. (1996). Keratinocyte growth factor (KGF) can replace testosterone in the ductal branching morphogenesis of the rat ventral prostate. *Int. J. Dev. Biol.* **40,** 941–951.

Tanaka, M., Komuro, I., Inagaki, H., Jenkins, N. A., Copeland, N. G., and Izumo, S. (2000). *Nkx3.1,* a murine homolog of Drosophila *bagpipe,* regulates epithelial ductal branching and proliferation of the prostate and palatine glands. *Dev. Dyn.* **219,** 248–260.

Thomas, R., Anderson, W. A., Raman, V., and Reddi, A. H. (1998). Androgen-dependent gene expression of bone morphogenetic protein 7 in mouse prostate. *Prostate* **37,** 236–245.

Thomson, A. A., and Cunha, G. R. (1999). Prostatic growth and development are regulated by FGF10. *Development* **126,** 3693–3701.

Thomson, A. A., Foster, B. A., and Cunha, G. R. (1997). Analysis of growth factor and receptor mRNA levels during development of the rat seminal vesicle and prostate. *Development* **124,** 2431–2439.

Timme, T. L., Truong, L. D., Merz, V. W., Krebs, T., Kadmon, D., Flanders, K. C., Park, S. H., and Thompson, T. C. (1994). Mesenchymal–epithelial interactions and transforming growth factor-β expression during mouse prostate morphogenesis. *Endocrinology* **134,** 1039–1045.

Vainio, S., Karavanova, I., Jowett, A., and Thesleff, I. (1993). Identification of BMP-4 as a signal mediating secondary induction between epithelial and mesenchymal tissues during early tooth development. *Cell* **75,** 45–58.

Warot, X., Fromental-Ramain, C., Fraulob, V., Chambon, P., and Dolle, P. (1997). Gene dosage-dependent effects of the *Hoxa-13* and *Hoxd-13* mutations on morphogenesis of the terminal parts of the digestive and urogenital tracts. *Development* **124,** 4781–4791.

Wilding, G. (1991). Response of prostate cancer cells to peptide growth factors: Transforming growth factor-β. *Cancer Surv.* **11,** 147–163.

Wilkinson, D. G. (1992). Whole mount in situ hybridization of vertebrate embryos. *In* "In Situ Hybridization: A Practical Approach" (D. G. Wilkinson, Ed.), pp. 75–83. Oxford University Press, Oxford, UK.

Winnier, G., Blessing, M., Labosky, P. A., and Hogan, B. L. M. (1995). Bone morphogenetic protein-4 is required for mesoderm formation and patterning in the mouse. *Genes Dev.* **9,** 2105–2116.

Wozney, J. M., Rosen, V., Celeste, A. J., Mitsock, L. M., Whitters, M. J., Kriz, R. W., Hewick, R. M., and Wang, E. A. (1988.). Novel regulators of bone formation: Molecular clones and activities. *Science* **242,** 1528–1534.

Yamashita, H., Ten Dijke, P., Heldin, C.-H., and Miyazono, K. (1996). Bone morphogenetic protein receptors. *Bone* **19,** 569–574.

Yan, G., Fukabori, Y., Nikolaropoulos, S., Wang, F., and McKeehan, W. L. (1992). Heparin-binding keratinocyte growth factor is a candidate stromal to epithelial cell andromedin. *Mol. Endocrinol.* **6,** 2123–2128.

Received for publication September 5, 2000
Revised December 30, 2000
Accepted January 18, 2001
Published online March 13, 2001